16th World Conference on Earthquake Engineering, 16WCEE 2017
Santiago Chile, January 9th to 13th 2017
Paper N° 2442
Registration Code: S- C1465324677

TSUNAMI RISK FOR CHILE'S COASTAL AREAS

A. Puelma,[1] B. Carrión,[2] and F. Medina[3]

[1] Principal Engineer, PRDW Consulting Port and Coastal Engineers, Santiago, Chile, apuelma@prdw.com
[2] Senior engineer, PRDW Consulting Port and Coastal Engineers, Santiago, Chile, bcarrion@prdw.com
[3] Principal, FME Engineering, San Francisco, California, USA, francisco@cal.berkeley.edu

Abstract

Chile is affected by destructive earthquakes; of these earthquakes, those occurring offshore have the potential to generate destructive tsunamis. To assess the risk of tsunami damage generated by subduction seismic events, several analyses have been conducted on eleven major Chilean coastal cities. From the characterization of five mega-thrust events occurring due to the subduction of the Nazca plate below the South American plate, Okada's rupture model is applied as the initial boundary condition to five regional numerical models representing massive water waves propagating towards the continent. The mega-thrust events were characterized to represent a code-level earthquake, but not the maximum historical earthquake (1960 Valdivia earthquake, Mw=9.5). Using the results of these five regional models as boundary conditions, eleven refined numerical models were used to compute the onshore water invasion and the velocity of impact on the infrastructure encountered. On both, regional and local models, the most accurate bathymetry of the ocean floor was used; similarly, the up-to-date coastline geometry, onshore topography, and infrastructure localization were included. The infrastructure was assumed to be reflective. The models were built and analyzed using state-of-the-art technology to represent the boundary conditions, water domains, seafloor bathymetry, and onshore topography and geometry, as accurately as needed. The models were successfully verified with data observed after the 2010 Maule earthquake (Mw=8.8). The results obtained indicated that most of the eleven cities studied were relatively safe from the destructive damage that these types of tsunamis generate, mostly due to the hilly geography of Chile's coastal region. However, the areas, and infrastructure on the coastline such as ports, would be subjected great damage. The eleven coastal cities studied were: Arica, Iquique, Mejillones, Antofagasta, La Serena, Coquimbo, Quintero, Viña del Mar, Valparaíso, San Antonio, and Talcahuano.

Keywords: Tsunami water-wave modeling, Tsunami inundation; Chile tsunami risk; Viña del Mar and Valparaíso tsunami.

1. Introduction

Continental Chile has been, and is, conditioned by the underlying tectonics associated to a convergent margin of tectonic plates, the most important being the subduction of the Nazca plate under the South American plate between Arica, from the north, and the triple junction close to the Taitao Peninsula, to the south. This subduction process has generated, and is capable of generating, seismic events of great magnitude, which in turn cause tsunamis with great damage potential along Chile's coastline, and even at distant sites like on the coasts of California, Hawaii and Japan, amongst others [1-2]. Two recent events standout: (1) the 1960 Valdivia earthquake, which generated the most important tsunami on Chile's coasts during the XX Century, in terms of damage and wave heights; and (2) the 2010 Maule earthquake, which generated the most recent tsunami and one of the most destructive that have occurred in Chile.

Eleven major coastal cities were studied: Arica, Iquique, Mejillones, Antofagasta, La Serena, Coquimbo, Quintero, Viña del Mar, Valparaíso, San Antonio, and Talcahuano. These cities are of interest because are characterized by: (a) high urban density next to the coastline; (b) residential, industrial, and governmental exposure to potential destructive tsunamis; and (c) negligible to non-existent infrastructure protection to the destructive effects of tsunamis. In addition to these cities, the entire Chilean coastline, from north to south, is subject to the effects of tsunami-genic seismic events. Thus, if the tsunami-genic event is of great magnitude, a large region of the Chilean coastline will be affected, impacting large urban areas as well as small towns.

Five tsunamis generated by an equal number of earthquakes were numerically modeled with resolutions of the order of 10 m: (a) on a regional scale, to include the effects of edge waves and trapped energy along the coastline; and (b) on a local scale, to characterize the inundation and the flow velocity field. The models and the methodologies used correspond to the state-of-the-art of tsunami simulation techniques. Maximum water heights and maximum velocity flow magnitudes were obtained in the inundated zones, on regular 100×100 m grids.

2. Data Sources and Methodology Background

2.1 Data sources

The bathymetric information used to build the models was obtained from the nautical charts published by the Chilean Navy Hydrographic and Oceanographic Service (*Servicio Hidrográfico y Oceanográfico de la Armada*, SHOA) [3], from the database maintained by the International Oceanographic Organization and UNESCO's Intergovernmental Oceanographic Commission (General Bathymetric Chart of the Oceans, GEBCO) [4], and bathymetric data from our own records. The topographic information was obtained from the elevation World model published by NASA (Shuttle Radar Topography Mission) [5], from Inundations Charts Due to Tsunami published by SHOA [6], and topographic data from our own records. The information on urban distribution of buildings and streets was obtained from Shoreline Maritime Plans published by SHOA [7], complemented and updated with digitized information from Google Earth satellite images.

2.2 Seismic events considered

Five seismic events with 150- to 255-year return periods were considered, conservatively assuming the subduction as a single probable event occurring anywhere over the length of the subduction interface. The associated seismic parameters are shown in Table 1. Note that these events are not as large as the 1960 Valdivia earthquake [8], considered close to a maximum credible earthquake.

Table 1 – Maximum probable earthquakes occurring on the regions of interest.

LOCATION	MAGNITUDE M_W	HYPOCENTER			FAULT			
		LONGITUDE (º)	LATITUDE (º)	DEPTH (km)	LENGTH (km)	WIDTH (km)	SLIP (m)	STRIKE (º)
Arica Iquique (5 sections)	9.0	-71.4	-18.6	30.4	100	150	12	330.0
		-71.1	-19.3		100	150	12	338.0
		-70.9	-20.0		100	145	12	346.0
		-70.7	-20.8		100	140	12	354.0
		-70.6	-21.5		100	140	12	0.0
Mejillones Antofagasta	9.0	-71.2	-23.2	27.8	400	140	15	8.0
La Serena Coquimbo	9.0	-72.3	-29.9	26.2	400	130	15	12.5
Quintero Viña del Mar Valparaíso San Antonio	9.0	-72.8	-32.9	26.8	400	140	15	10.0
Talcahuano	9.1	-74.4	-36.4	29.0	400	160	15	15.0

2.3 Initial deformation

A large subduction tsunami-genic earthquake releases large amounts of energy, generated by the relative displacement of the tectonic plates as the rupture propagates from the asperities in the interface to the crust surface on the seabed. This process displaces the sea water vertically on a wave that propagates in compression from the seabed to the surface of the ocean, triggering a tsunami, that in the case of Chile exhibits water waves propagating to: (a) the east, greatly impacting the coastline a few minutes after the earthquake occurs; (b) the north, impacting the coastline of the rest of the Americas, from few to several hours after occurrence; and (c) the west, impacting from the Pacific Ocean islands to the coastline of Asia, from several hours to close to a day after occurrence. Considering the time scale of the tsunami versus that of the crust deformation, the crustal vertical displacement is assumed instantaneous and transferred to the water column above, up to the free surface, without loss of energy. The vertical perturbation is proportional to the crustal area activated during the seismic event, and is propagated in all directions by the ocean water with a celerity of hundreds of km/hr. Since the fault outcrops at the Peru-Chile trench, a few kilometers offshore and approximately parallel from Chile's coastline, the tsunami waves arrive a few minutes after the fracture without the benefit of radial attenuation.

Okada's close-form solution [9] was used to generate the initial perturbation on the ocean free surface (as example, see Fig. 1), by calculating the crust deformations from the fault macro seismic parameters. Once the ocean free surface initial deformation is generated, the perturbation is propagated as a linear wave of small amplitude and large wavelength at sufficiently large depths. When the wave comes close to the coast, nonlinear interactions amongst the celerity, the sea level, the local depth, and the coastline begin to be important. The numerical solution was obtained using MIKE 21 [10].

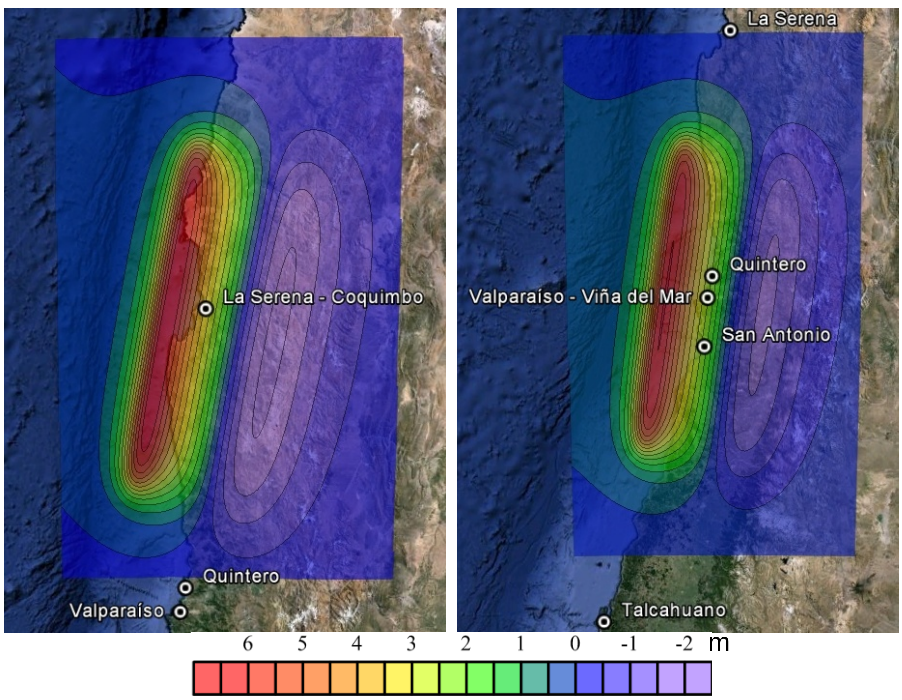

Figure 1 –Deep-water model initial conditions in front of La Serena and Coquimbo (left panel), and in front of Quintero, Valparaíso-Viña del Mar, and San Antonio (right panel).

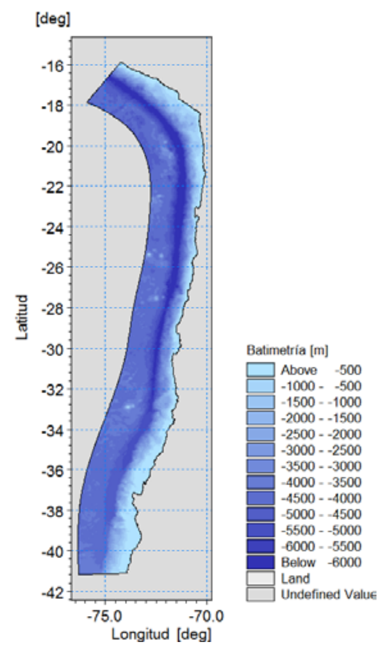

Figure 2 – Domain used to model Chile's offshore tsunami wave propagation at a regional scale.

2.4 Numerical modeling of water waves

Given that the processes at large- and shallow-water depths exhibit different physical characteristics, and different time and distance scales, they were modeled independently, utilizing the results from the models at regional scale, or large-water depths, as boundary conditions to the local-scale, or shallow-water depths models. The open ocean water propagation was modeled using MIKE 21 [11], solving the hydrodynamic equations by means of the finite volume method. The geometric domains defined for the regional models were 25° (~2.900 km), along the north-south direction, and a variable width between 250 and 300 km, on the east-west direction, depending on the distance between the Peru-Chile trench and the continent. The domains to the west of the trench were extended approximately 100 km (Fig. 2). The shallow-water nonlinear equations were solved averaging over the vertical coordinate, considering the Coriolis and seabed friction effects. The mesh has a resolution of approximately 3 km. The boundary conditions on the coastline are closed with a normal velocity equal to 0, otherwise are open with velocity equal to 0 in both axes (Flather's condition [12]). The total elapsed time of the simulation was approximately 5 hours, for a 10 s time interval.

2.5 Numerical modeling of inundation

The local propagation and the wave interaction with the coastline were modeled using the computational program ANUGA [13], solving the shallow-water hydrodynamic equations and capturing the nonlinear interaction effects. The models considered the existence of the coastline, separating the domain in two zones, one active in the presence of water, and another inactive remaining dry. The interaction between both zones is hydraulically and numerically complex. ANUGA treats this interaction with an *ad-hoc* numerical procedure. A grid was built for each local model that, in addition to the bathymetric and topographic data, it included information respect to the urban distribution of buildings and streets (Figs. 3 and 4).

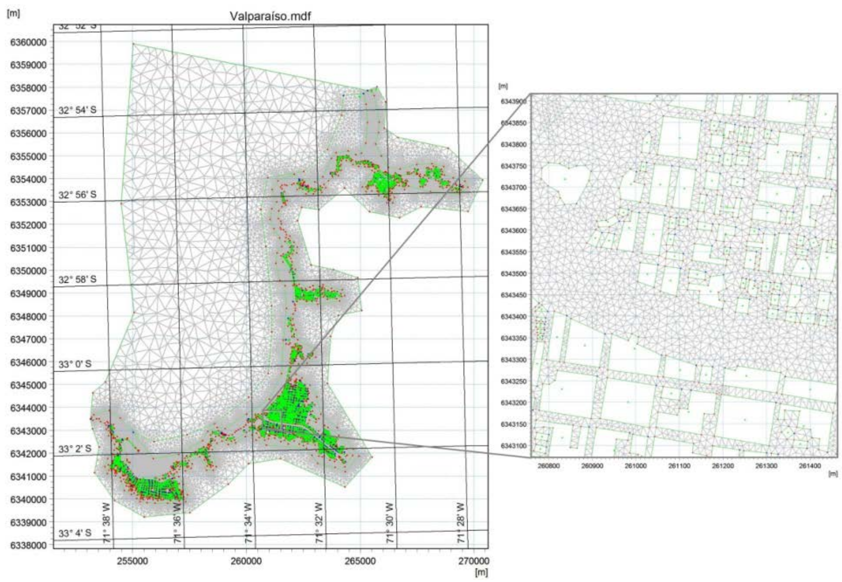

Figure 3 – Spatial distribution resolution in the ANUGA model for Viña del Mar and Valparaíso.

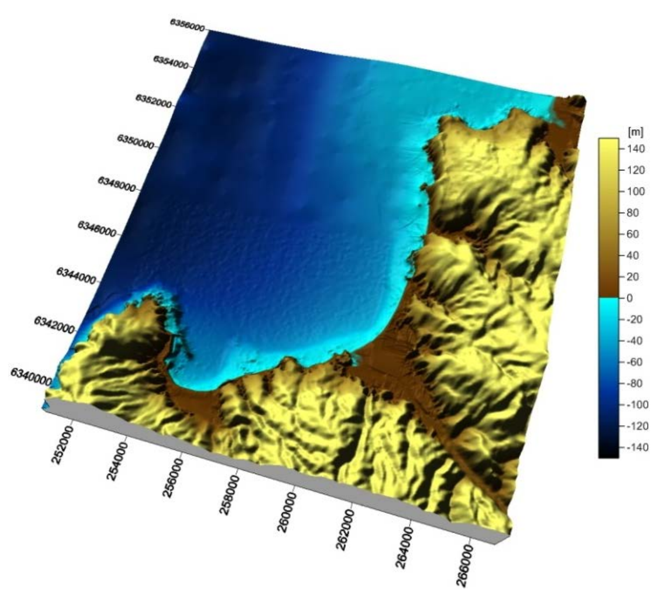

Figure 4 – Topo-bathymetry used in the ANUGA model domain for Viña del Mar and Valparaíso.

3. Methodology Validation

The methodology described was compared to data measured and observed in the field after the 2010 Maule earthquake, obtaining good correlation between the results from the models and the field data.

3.1 Arrival times

The near field results were compared with available data on wave arrival times reported along the coastline. These times were published by the press [14], citing research sources in the Chilean Navy's General Directorate for Maritime Territory and Merchant Marine and in SHOA. The information published shows approximate arrival times on six sites (Fig. 5) located on the most affected regions such as Constitución, Dichato, Talcahuano, and the Juan Fernández Archipelago, in addition to important ports such as Valparaíso and San Antonio, where tide gauges recorded the event. A good correlation is observed between the arrival times reported and those of the calculated time series, shown as blue lines over the press infographic. Results for San Antonio and Pichilemu are not shown because they were not part of the evaluations carried out on this project. The model represents adequately the hydrodynamics of the tsunami waves in deep waters.

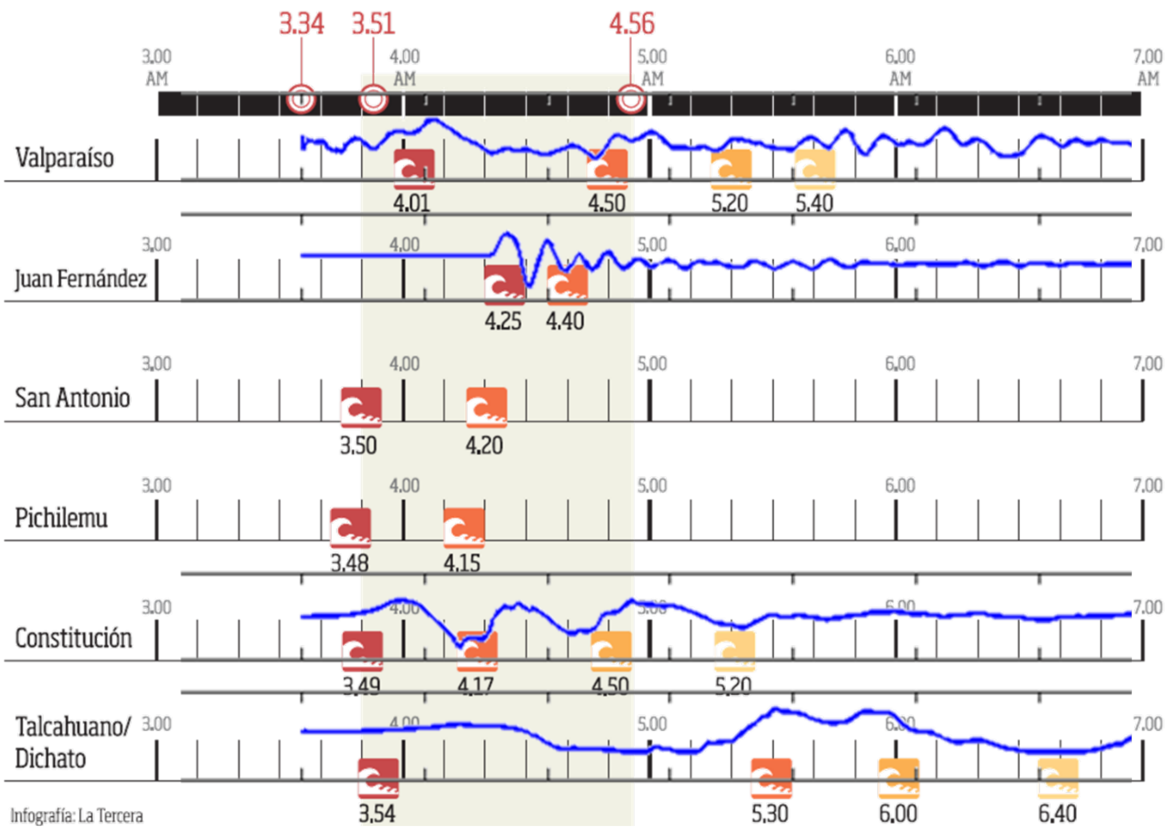

Figure 5 – Comparison between computed results and data published by the press [14] for the 27 February 2010 Maule earthquake and tsunami.

3.2 Tsunami tide record

Concepción Bay was locally modeled with ANUGA, using the results obtained with the MIKE 21 regional model as data entry. Results from the local model were compared with a record measured by a tide gauge located at the interior of a dock owned by the Chilean Navy's Shipbuilding and Ship Repair Company (*Astilleros y Maestranzas de la Armada de Chile, ASMAR*) in Talcahuano [15]. On Fig. 6 it is observed that the model correctly represents the first-wave arrival time and amplitude. The instrument did not measure the valley, since the free surface decreased to below the instrument zero (dry condition). The arrival of the second wave is correctly represented just before the instrument ceased operating. The arrival time and the slenderness of the wave of this second front are in good agreement with the measured record. The small wave out-of-phase observed, approximately 7 minutes, could be due to the updated (2013) bathymetry used in the model.

Figure 6 – Comparison between a time series recorded by a tide gauge (red line), located on an ASMAR dock in Talcahuano [15], and results computed (blue line) for the 27 February 2010 Maule earthquake and tsunami.

4. Results

Results for the five seismic events modeled at regional scale and their impact on the eleven cities studied were obtained and are presented in detail elsewhere [16]. A brief summary of the measurable effects on the modeled tsunamis over the locations studied is shown in Table 2.

Table 2 – Effects of the modeled tsunamis over the locations studied.

CITY	NUMBER OF WAVES[a]	WAVE ARRIVAL		MAXIMA			COMMENTS
		FIRST	LAST[a]	RUN-UP[c]	INUNDATION DEPTH[d]	HORIZONTAL PENETRATION[c]	
		(min)	(min)	(m NRS)	(m)	(m)	
Arica	6	24	253	25	16	2,670	Largest inundation: area north of city. Civic center inundated.
Iquique	5	14	110	20	8	750	Largest inundation: free-trade zone. Civic center partially inundated.
Mejillones	5	5	245	18	12	400	Largest inundation: urban area. Industrial area on coastline affected.
Antofagasta	7	9	275	18	9	750	Largest inundation: civic center. Some inundation on north and south areas.
La Serena	10	10	257	20	16	2,300	Large inundation in front of La Serena, concentrated to the west of Route 5. Civic center not affected.
Coquimbo Centro							Large inundation in Coquimbo civic center.
Coquimbo and Herradura de Guayacán							Inundation weaker than in Coquimbo bay, concentrated in the lowland area, west of Route 5.
Quintero	8	15	157	27	14	1,980	Largest inundation: Air Force base and Campiche Creek area. Industrial areas close to the creek more affected than those located to the south.
Viña del Mar	4	14	125	25	10	3,190	Largest inundation: Marga Marga Creek riverbed and neighboring areas. Reñaca creek allows large water penetration.
Valparaíso							Inundation from Pedro Montt Avenue to the north and all the city plan, from Victoria Plaza to the west.
San Antonio	3	15	110	20	10	3,000	Civic center is not affected much. Maximum water penetration occurs at the Maipo River box.
Talcahuano	4	38	453	18	11	2,350	Large part of the city is inundated, from Concepción Bay on the north and from the San Vicente Bay on the southwest. The airport tarmac is not inundated; the surroundings are.

NOTES:

[a] Number of relevant waves: waves that on the control point of each city exceed 3 m over MSL.

[b] Wave arrival time: elapsed time for a wave to reach maximum elevation.

[c] Run-up and maximum penetration: extreme values, do not represent the mean behavior in a given location.

[d] Maximum inundation depth: measurement over the coastline.

In general, the sites exhibit different responses. The maximum inundation elevations reached for all the sites are bounded at +15 m, while maximum magnitude of water flow velocities vary from 6 to 15 m/s. The inundation areas calculated vary depending on the site. In cities located on relatively highland areas like Antofagasta and Mejillones, the inundations observed are moderate, while on lowland cities like La Serena and Talcahuano, the inundations observed are significant. A sample of the results obtained for Viña del Mar and Valparaíso are subsequently presented.

4.1 Regional model: Quintero, Viña del Mar, Valparaíso, and San Antonio

To illustrate the regional dynamics of the event, Fig. 7 shows maps with ocean levels for times t = 0, 5, 10, 20, 40, and 60 minutes. For t=0, the initial perturbation of the sea is aligned with the Peru-Chile trench. Propagation starts perpendicularly along the fault; that is, towards Chile's coastline and the Pacific Ocean. After 10 minutes of occurrence, it is observed that the first front has reached its maximum expression in Quintero and Valparaíso, and is close to reach San Antonio. At the 20-minute mark, a first sea-level decline is observed, and at the 60-minute mark, there is an ascent.

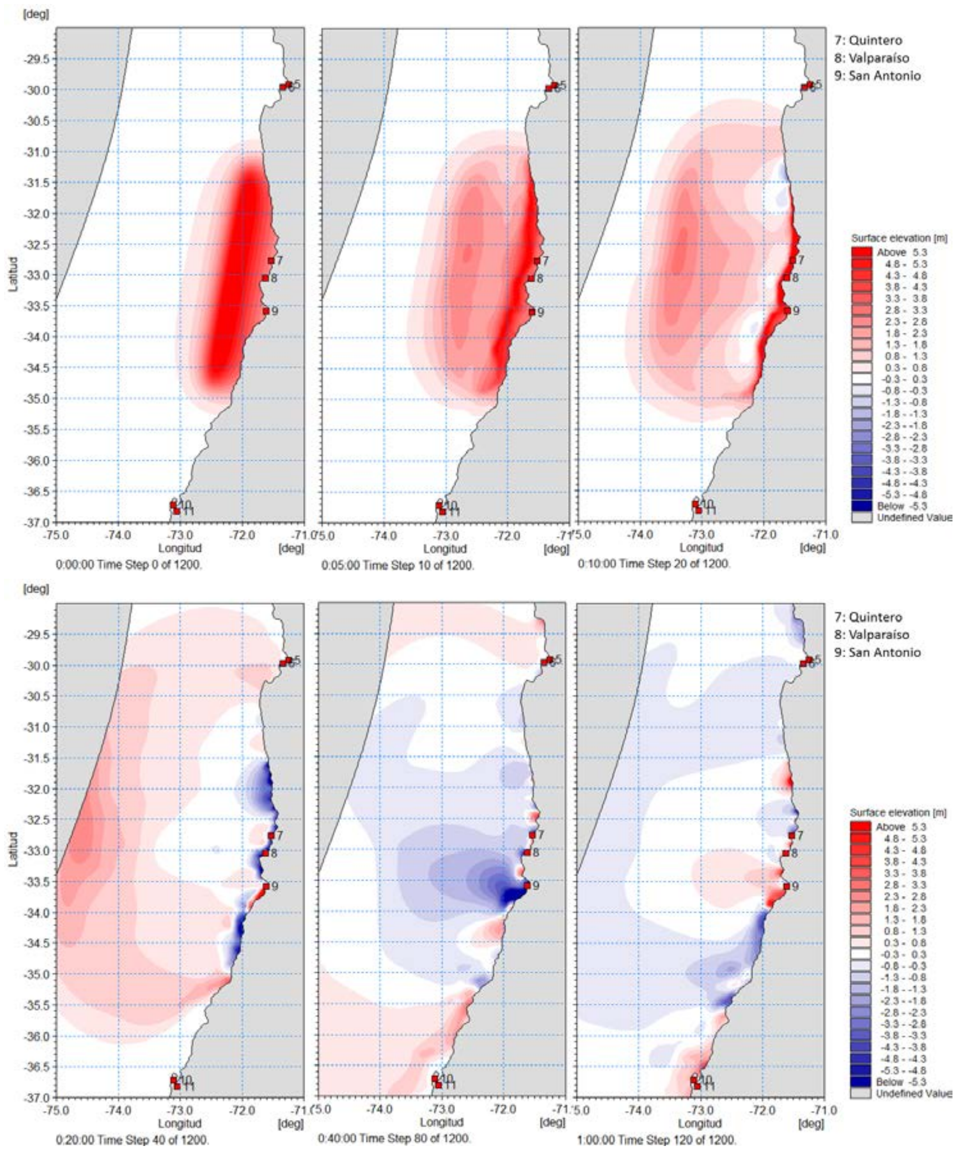

Figure 7 – Coastal wave evolution for a regional seismic event modeled for Quintero, Viña del Mar, Valparaíso, and San Antonio. Post-event times: 0, 5 and 10 minutes (upper panels), and 20, 40 and 60 minutes (lower panels).

Fig. 8 shows several points close to the local domain boundaries. Fig. 9 shows the record at the border of the Viña del Mar domain model. The larger waves are concentrated in the first 90 minutes, with a main frontal energy and two secondary waves, most likely due to energy trapped at the coastline. Then, the wave height declines. The second and fourth waves are more significant in Valparaíso. In this case, the first effect is a sudden upsurge of the sea surface elevation. This observation goes against the popular belief that the sea level always descends first, giving notice to the observer that a wave crest is coming soon after.

Figure 8 – Nodes in the regional model used to interpolate the local model boundary conditions for Viña del Mar-Valparaíso.

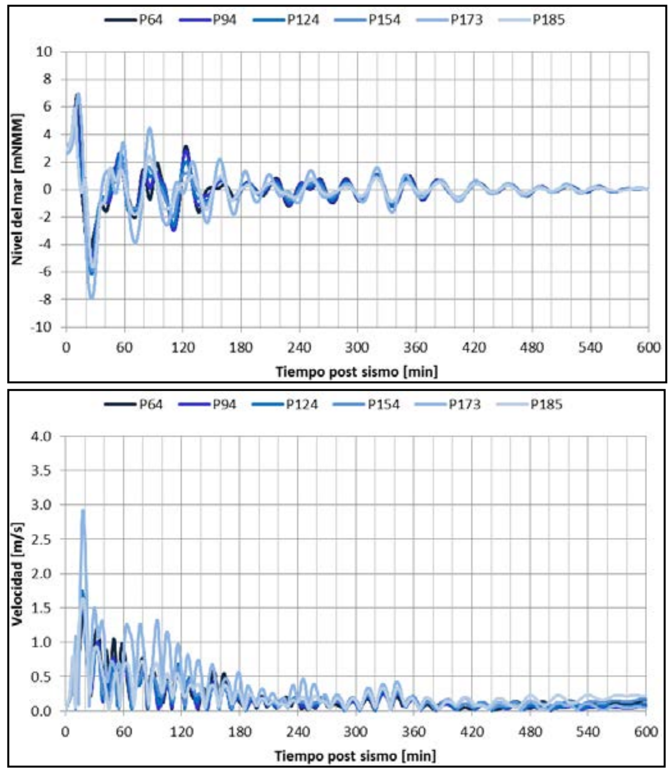

Figure 9 – Time series of sea level (upper panel) and velocity amplitude (lower panel) on the nodes shown on Fig. 7 for Viña del Mar-Valparaíso.

4.2 Local model: Viña del Mar - Valparaíso

Fig. 10 shows the maximum inundation depth in Viña del Mar; a detail is shown on Fig. 11.

Figure 10 – Inundation depth: Viña del Mar.

Figure 11 – Inundation detail: Viña del Mar urban center.

On the coastline, 10-m depths are observed. The maximum water penetration occurs on the Marga Marga Creek course reaching over 3 km inland. The Reñaca Creek course also allows an incursion above the average, reaching over 1 km horizontally. It is observed an inundation depth over 8 m around the Casino and between 4 and 6 m around the Municipality. Center areas exhibit a significant inundation.

In the case of Valparaíso (Figs. 12 and 13), the inundation depth over the coastline is above 8 m, not as high as in Viña del Mar, reaching a maximum water penetration of 600 m on Argentina Avenue. It can be observed that west of Victoria Plaza the inundation covers the entire city plan, whereas to the east it does not go beyond Pedro Montt Avenue.

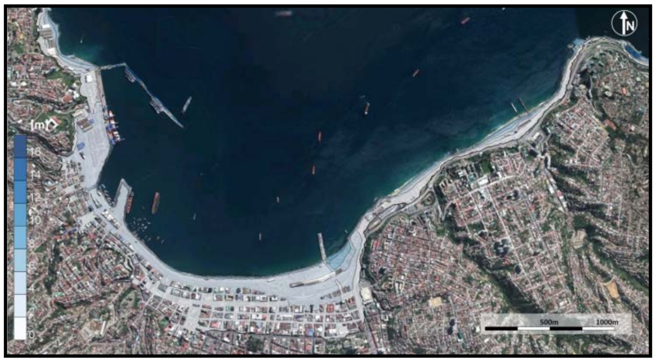

Figure 12 – Inundation depth: Valparaíso.

Figure 13 – Inundation detail: Valparaíso urban center.

Figs. 14 and 15 show the maximum inundation velocities for Viña del Mar and Valparaíso, respectively. It can be observed that on Viña del Mar beach the velocities reach 10 m/s, while at the first building row, the values are between 3 and 4 m/s. In Valparaíso, it is observed that on the coastline maximum velocities are about 5 m/s, and about 3 m/s, at the first building row. Over the Valparaíso breakwater, the velocities are much higher.

Figure 14 – Maximum inundation velocities: Viña del Mar.

Figure 15 – Maximum inundation velocities: Valparaíso.

Fig. 16 shows the times series corresponding to the sea level and the velocity vector amplitude on a point located on the Port of Valparaíso breakwater. It is observed that it resembles the deep-water record shown on Fig. 9, except for a small increase of the wave amplitude. The maximum velocity occurs during the first wave withdrawal (backwash). After two hours from the event occurrence, the velocities are below 1 m/s.

To further understand the process, simulations of the tsunamis impacting all modeled cities were recorded. The simulation for Viña del Mar, generated by the offshore earthquake shown in Table 1, can be activated on Fig. 17, where it can be observed that the average flood incursion is about 500 m from the coast line. However, the Marga Marga Creek facilitates the flooding farther, inundating areas such as the downtown, the main city plaza, the southern end of Libertad Avenue, and also the vicinity of the Sporting Club, about 2 km inland.

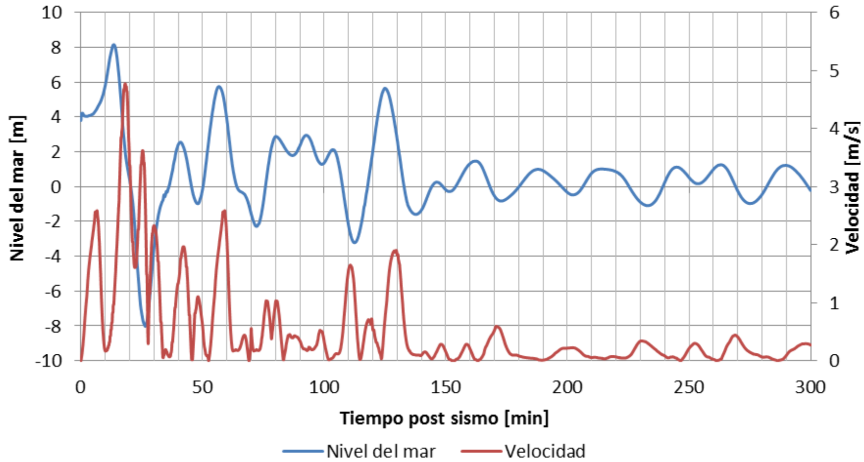

Figure 16 – Time series of sea level and vector velocity amplitude computed on a point [71º37'05" W; 33º01'56" S; -14.4 m *NRS*†] close to the Port of Valparaíso breakwater.

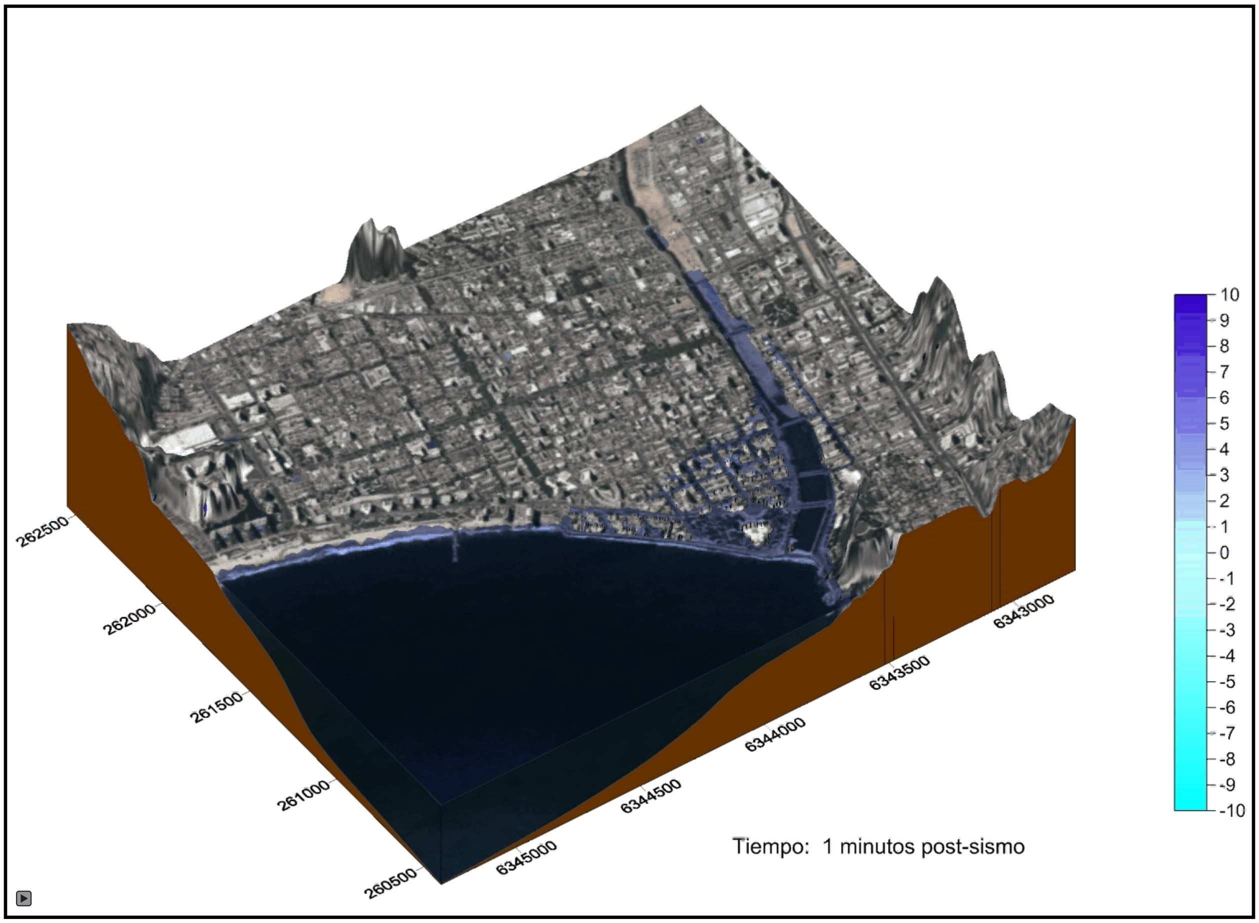

Figure 17 – Tsunami impacting the city of Viña del Mar, generated by an offshore maximum probable earthquake.

†*NRS*: *Nivel de Reducción de Sonda*s (Soundings Reduction Level), corresponding to Chile's Chart Datum (CD).

5. Conclusions

From the eleven cities studied, and the observed results, the following conclusions are obtained:

- Due to their differentiated geomorphology (orientation, bathymetry, and topography) and development level (built area density), all studied sites responded differently.
- Maximum inundation depths occur at the coastline and are generally below 15 m. However, the run-up can reach and surpass +20 m *NRS*, usually adopted as a safe elevation.
- The first wave arrival time is in the 5- to 40-minute range, mostly depending on the epicenter location. In some cases,there might not be enough time for a proper and complete evacuation.
- The flow maximum velocities are generally between 6 to 15 m/s in the coastline, whereas they are approximately 5 m/s at the first building row.
- The presence of watercourses facilitates the intrusion of the flow inland, producing inundations due to the lateral overflow.
- If high tide is to be considered at the time of the event, the expected maximum inundation level could be up to 1.0 m greater than the results obtained considering average tide.
- The results, in general, present inundations similar to those shown by SHOA's inundation charts [6], with notable differences only in the cases of Iquique and Mejillones, where SHOA predicts greater inundations. Considering that the seismic event modeled by SHOA in both cases is of lesser or equal magnitude to the one modeled in this study, the difference could be found in the topo-bathymetric information or in the characterization of the ocean-floor dislocation generating the tsunami.
- At the considered earthquake magnitudes analyzed, it was observed that the most vulnerable cities are: Arica, Mejillones, Quintero, Viña del Mar, Valparaíso, San Antonio, and Talcahuano, in no special order.
- In harbors, filtering and resonance effects were observed; the most notable case is Concepción Bay; however, Mejillones, Antofagasta, Coquimbo, and Quintero show marked oscillations.

6. Acknowledgements

The sponsorship of the Association of Chilean Insurers (*Asociación de Aseguradores de Chile*) is gratefully acknowledged. Dr. Harry Yeh and Dr. Phillip Watts provided valuable comments.

7. References

[1] Lockridge PA (1985): 'Tsunamis in Peru-Chile,' *report SE-39*, World Data Center A for Solid Earth Geophysics, Boulder, Colorado, USA.

[2] Barrientos SE (2011): 'Grandes tsunamis que han afectado las costas de Chile,' en La Sismología en Sudamérica y los Mecanismos de Prevención y Mitigación del Peligro y Riesgo Sísmico. Homenaje a Alberto Giesecke (D Huaco, editor), 147-152, Asociación Andrés del Castillo y Centro Regional de Sismología para América del Sur (CERESIS), Lima, Perú.

[3] SHOA (1979-2002): *Carta Náutica*, misc. numbers, misc. scales, Servicio Hidrográfico y Oceanográfico de la Armada, Valparaíso, Chile. {http://www.shoa.cl/pagnueva/cartaspapel.html} [March 2013]

[4] GEBCO (2013): *The GEBCO_08 Grid*, version 20031120, General Bathymetric Chart of the Oceans, Intergovernmental Oceanographic Commission, UNESCO. {http://www.gebco.net/data_and_products/gridded_bathymetry_data/} [04 March 2013]

[5] Farr TG, Rosen PA, Caro E, Crippen R, Duren R, Hensley S, Kobrick M, Paller M, Rodriguez E, Roth L, Seal D, Shaffer S, Shimada J, Umland J, Werner M, Oskin M, Burbank D, Alsdorf D (2007): 'The Shuttle Radar Topography Mission,' *Reviews of Geophysics*, **45**, RG2004.

[6] SHOA (2000-2013): *Carta de Inundación por Tsunami*, misc. numbers, misc. scales, Servicio Hidrográfico y Oceanográfico de la Armada, Valparaíso, Chile. {http://www.snamchile.cl/} [March 2013]

[7] SHOA (2001-2006): *Plano Marítimo del Borde Costero*, misc. numbers, misc. scales, Servicio Hidrográfico y Oceanográfico de la Armada, Valparaíso, Chile. {http://www.shoa.cl/pagnueva/planos_borde_costero.html} [March 2013]

[8] Lomnitz C (2004): 'Major earthquakes of Chile: A historical survey, 1535-1960,' *Seismological Research Letters*, **75**, 368-378.

[9] Okada Y (1985): 'Surface deformation due to shear and tensile faults in a half-space', *Bulletin of the Seismological Society of America*, **75**, 1135-1154.

[10] DHI Group(2012): *MIKE 21 Toolbox. User Guide*, Danish Hydraulic Institute, Hørsholm, Denmark.

[11] DHI Group (2012): *MIKE 21 Flow Model FM. Hydrodynamic Module. User Guide*, Danish Hydraulic Institute Group, Hørsholm, Denmark.

[12] Flather RA (1976): 'A tidal model of the north-west European continental shelf,' *Memoires de la Société Royale des Sciences de Liège*, **6**, 141-164.

[13] Nielsen O, Roberts S, Gray D, McPherson A, Hitchman A (2005): 'Hydrodynamic modelling of coastal inundation,' *MODSIM 2005: International Congress on Modelling and Simulation*, (A Zerger and RM Argent, editors), 518-523, Modelling and Simulation Society of Australia and New Zealand (2005).

[14] La Tercera Edición Impresa (2010): 'Desastre causó grave daño a red de alerta de tsunamis', 16 (26 March 2010).

[15] IOC (2012): 'Station: Talcahuano_CL,' *Sea Level Station Monitoring Facility*, Intergovernmental Oceanographic Commission, UNESCO, Paris, France.

[16] PRDW Aldunate Vásquez and FME Engineering (2015): *Proyecto Mapa de Riesgo Sísmico de Chile. Módulo 3: Riesgo por Tsunami*, informe para Asociación de Aseguradores de Chile, FME Engineering, San Francisco, California, USA (21 March 2015).